JACS
JOURNAL OF THE AMERICAN CHEMICAL SOCIETY
Article
pubs.acs.org/JACS

Toward Oriented Surface Architectures with Three Coaxial Charge-Transporting Pathways

Giuseppe Sforazzini, Edvinas Orentas,† Altan Bolag, Naomi Sakai, and Stefan Matile*

Department of Organic Chemistry, University of Geneva, Geneva, Switzerland

Supporting Information

ABSTRACT: We report a synthetic method to build oriented architectures with three coaxial π-stacks directly on solid surfaces. The approach operates with orthogonal dynamic bonds, disulfides and hydrazones, self-organizing surface-initiated polymerization (SOSIP), and templated stack-exchange (TSE). Compatibility with naphthalenediimides, perylenediimides, squaraines, fullerenes, oligothiophenes, and triphenylamine is confirmed. Compared to photosystems composed of two coaxial channels, the installation of a third channel increases photocurrent generation up to 10 times. Limitations concern giant stack exchangers that fail to enter SOSIP architectures (e.g., phthalocyanines surrounded by three fullerenes), and planar triads that can give folded or interdigitated charge-transfer architectures rather than three coaxial channels. The reported triple-channel surface architectures are as sophisticated as it gets today, the directionality of their construction promises general access to multichannel architectures with multicomponent gradients in each individual channel. The reported approach will allow us to systematically unravel the ultrafast photophysics of molecular dyads and triads in surface architectures, and might become useful to develop conceptually innovative optoelectronic devices.

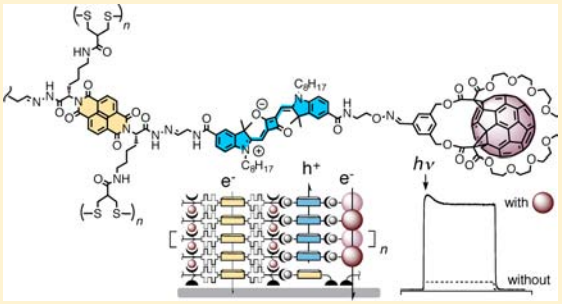

INTRODUCTION

In nature, functional systems have complex structures of highest sophistication.[1] Little is known about what we would get from similarly sophisticated organic materials, probably because of the lack of general synthetic methods to prepare them. This is still the case despite the promise of such methods to open the door to the materials of the future and much efforts worldwide to tackle this fundamental challenge in organic synthesis.[2−10] To contribute to these efforts, we became interested in the development of synthetic methods to grow functional multicomponent architectures directly on solid surfaces. Such methods are necessary to build functional systems with oriented gradients for cascade processes as in biological systems. Our initial attempts with zipper assembly, although successful, were synthetically too demanding to ensure rapid progress toward general use.[11] Facile access to complex systems, without extensive synthetic effort, was finally secured with self-organizing surface-initiated polymerization (SOSIP).[12]

For SOSIP, propagators **X1** are recognized by initiators **X2** or growing polymers on solid surfaces (Figure 1). Both **X1** and **X2** contain a central aromatic core that is expected to form functional, charge-transporting π-stacks in the final SOSIP architectures **X**. These functional channels are embedded in self-organizing, hydrogen-bonded networks from peptide-like structures. Initiators further contain diphosphonate groups to bind to indium tin oxide (ITO) surfaces and thiolates to initiate the polymerization. For ring-opening disulfide-exchange polymerization, propagators **X1** are equipped with strained cyclic disulfides. The envisioned combination of self-organization with weak noncovalent interactions and polymerization with dynamic covalent disulfide exchange chemistry[13] implements central lessons from protein chemistry. The obtained ladderphane[14] architecture **X** has been realized for central stacks of naphthalenediimides (NDIs),[12] perylenediimides (PDIs),[15] and oligothiophenes.[16,17]

To expand the SOSIP approach toward more complex architectures, templated self-sorting (TSS)[18] and templated stack exchange (TSE)[16,17,19,20] have been developed. In TSS, initiators are used as templates on the surface to grow uniform stacks next to each other by co-SOSIP. This transcription of information from 2D monolayers into 3D architectures can be achieved with up to 97% fidelity.[18] In TSE, the covalent counterpart to TSS, SOSIP architectures are grown in the presence of templates on the surface and along the π-stack.[19] The templates along the SOSIP stack are attached with a hydrazone bridge,[21] that is a covalent dynamic bond[22] orthogonal to the disulfides[13] in **X**. The templates along the SOSIP stack are then removed with hydroxylamine, and the empty space left behind in architectures **X3** is filled with aldehydes **Y** of free choice. The result is a double-channel architecture **XY**, characterized by two coaxial stacks of different nature. We have demonstrated successful construction of such double-channel architectures with NDIs,[19] triphenylamines,[19] PDIs,[16] fullerenes,[17] phthalocyanines,[20] and porphyrins[20] as the second channel.

Received: June 9, 2013
Published: August 1, 2013

dx.doi.org/10.1021/ja405776a | J. Am. Chem. Soc. 2013, 135, 12082−12090

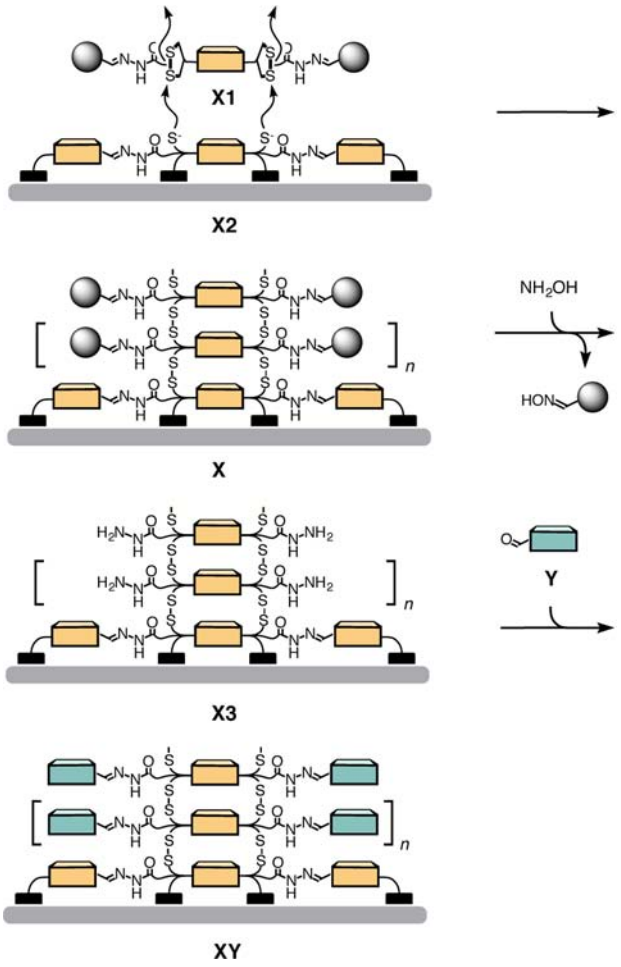

Figure 1. The SOSIP-TSE approach to double-channel surface architectures. Disulfide-exchange SOSIP yields the single-channel architecture **X**, TSE with chemo-orthogonal hydrazone exchange yields the double-channel architecture **XY**.

Nanostructured double-channel architectures are of interest in artificial photosystems because the coaxial alignment of transport pathways for electrons (e, n) and holes (h, p) with the width of molecules is expected to ensure efficient photoinduced charge separation at the maximized contact area, whereas charge mobility in the separate channels should remain high. Such architectures are referred to as supramolecular n/p-heterojunctions (SHJs).[2,23] Whereas several elegant approaches to SHJs have been reported in the recent literature, SOSIP-TSE is unique in the sense that it provides orientational control of SHJs relative to the surface. This directionality is essential to engineer antiparallel redox gradients into both channels.[19,20] Oriented antiparallel gradients (OMARGs) are expected to drive holes and electrons in opposite directions after their generation upon irradiation, a bit like in biological photosystems.[1] Already two-component gradients in OMARG-SHJ photosystems made by SOSIP-TSE were sufficient to significantly reduce charge recombination efficiencies.[19,20]

At this point, "triple-channel" photosystems **XYZ** were the obvious next big step to take toward architectures with higher complexity (Figure 2). The term "triple-channel" is used here to refer to architectures **XYZ** that are likely to contain three coaxial charge-transporting pathways. This is done for convenience only. Moreover, it is understood that all reported surface architectures will naturally contain defects. However, experimental evidence exists that the dynamic covalent chemistry used for SOSIP-TSE can minimize these defects by self-repair.[12] Triple-channel photosystems were fascinating because they offer as surface architectures what has been appreciated for decades as molecular triads[24] in solution. Better coverage of the solar spectrum as well as the long-lived charge separation due to stepwise electron transfer are some of the most attractive characteristics of triads. So far, little is known on molecular triads in surface architectures,[5j] presumably because general preparation methods were not available. In the following, we describe our attempt to synthesize triple-channel architectures containing several classical components of optoelectronic systems, that is NDIs,[3] PDIs,[4] oligothiophenes,[5] fullerenes,[6] squaraines,[7] phthalocyanines or porphyrins,[8] and triphenylamines[10] (Figure 2). The results reveal exceptional structural tolerance of the SOSIP-TSE approach and high functional importance of the newly introduced third channel. The main limitations concern giant stack exchangers and completely planar triads; the best activities were obtained for triad photosystems composed of NDIs, squaraines and fullerenes (Figure 3) or NDIs, PDIs and triphenylamines.

RESULTS AND DISCUSSION

General Design. The synthesis of triad photosystems **XYZ** was based on single-channel SOSIP architectures **A** with NDI stacks (Figure 2). This selection was made because SOSIP with NDI stacks is best understood. With a low-lying LUMO, this central NDI stack can also act as an electron-transporting channel in triple-channel architectures (Figure 2, bottom left). To secure the necessary space next to the NDI stacks for incoming stack exchangers, NDI templates on the ITO surface were used because they were shown to occupy enough space to allow nearly quantitative TSE of stack exchangers as large as phthalocyanines, and function as hole blockers.[20] Such size tolerance is counterintuitive but understandable considering that with two NDI templates per initiator the space reserved for TSE is more than twice as large as that occupied by one central NDI.

Along the channel **X** obtained from SOSIP, channel **Y** is attached using the hydrazone chemistry developed for TSE (Figure 2). This study focuses on triad architectures **XYZ** with squaraines **B**,[7] phthalocyanines **C**,[8] and PDIs **D**[4] in channel **Y**. Phthalocyanines **C** are green chromophores with properties similar to chlorophyll. Squaraines **B** have been introduced more recently as a more compact, better soluble phthalocyanine mimic. With a high-lying HOMO, squaraines **B** and phthalocyanines **C** are hole transporters. The complementary triad architecture with an electron-transporting channel in the middle was explored with the red PDI **D**.

Along this second channel **B**, **C**, or **D**, channel **Z** is attached via an oxime bridge (Figure 2). As oximes are more stable relatives of hydrazones,[25] formation of dyads **YZ** followed by TSE with SOSIP architecture **X3** should give the triad architecture **XYZ** without problem. Hole-transporting squaraines **B** and phthalocyanines **C** in channel **Y** are combined with electron transporters in channel **Z**. In the fullerene **E**, this powerful electron acceptor is wrapped in solubilizing TEG-tails.[17] The planar, core-expanded NDI **F** has attracted some recent attention because a very low LUMO is combined with a red-shifted absorption and excellent charge mobility in FETs.[3e] With electron-transporting PDI **B** in channel **Y**, hole transporters were placed in channel **Z**. A slightly deplanarized

dx.doi.org/10.1021/ja405776a | J. Am. Chem. Soc. 2013, 135, 12082−12090

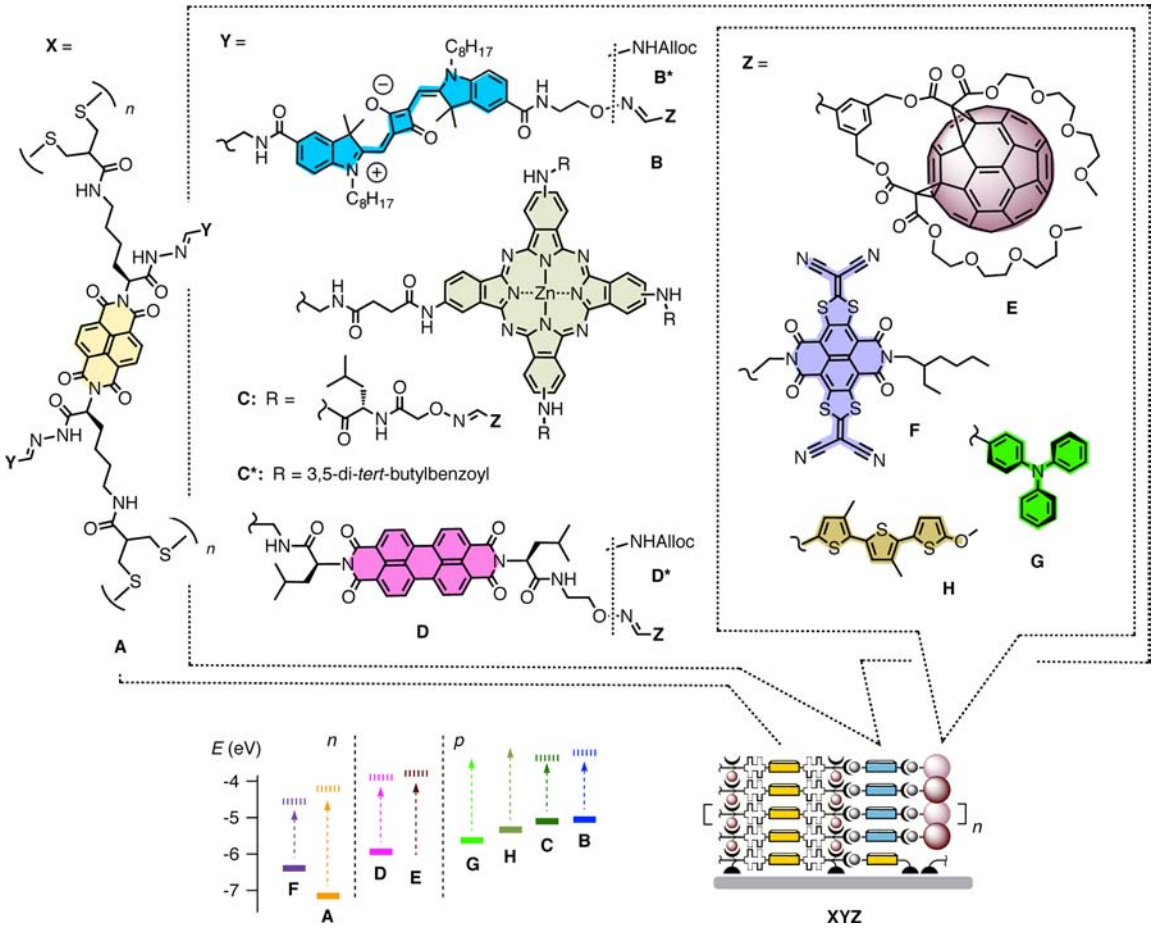

Figure 2. Triad architectures **XYZ** explored in this study, with energy levels of HOMO (bold) and LUMO (dashed) of electron (n) and hole (p) transporting components (in eV against vacuum, normalized for −5.1 eV for Fc/Fc^+).

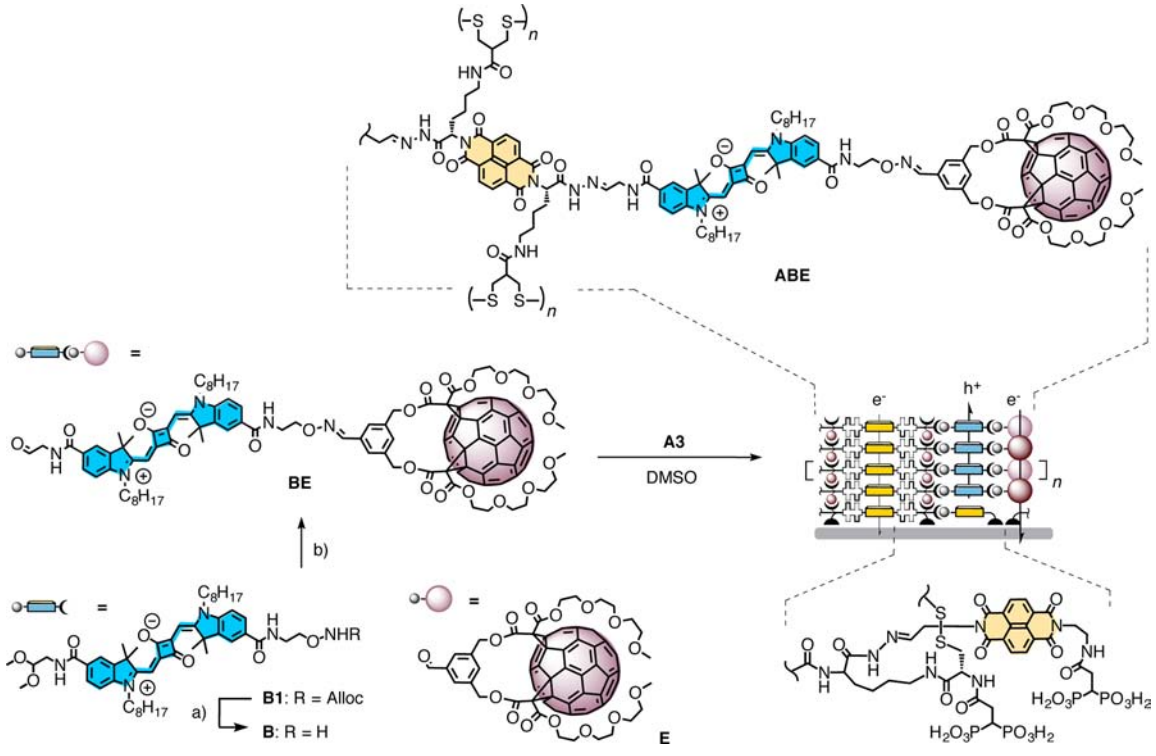

Figure 3. Synthesis and full structure of triple-channel architecture **ABE**. (a) $Pd(PPh_3)_2Cl_2$, *n*-Bu_3SnH, *p*-NO_2 phenol, (b) TFA.

dx.doi.org/10.1021/ja405776a | J. Am. Chem. Soc. 2013, 135, 12082−12090

oligothiophene **H**[5i] is compared with a nonplanar triphenylamine **G**.[10]

Triad Architectures with Squaraines and Fullerenes. Squaraines **B** have never been used before in SOSIP-TSE architectures. To serve as central channel **Y** in triple-channel architectures **XYZ**, the squaraines had to be equipped with a protected alkoxyamine on one side for the covalent capture of channel **Z** and an orthogonally protected aldehyde on the other side for TSE with the single-channel SOSIP architecture **X** (Figure 3). In squaraine **B1**, Alloc and acetal protection are used for this purpose. Squaraine **B1** was readily accessible by the coupling of the known dicarboxylic acid[7b] with the corresponding amines. Pd-mediated Alloc removal yielded the desired squaraine **B**. Oxime formation with fullerene **E** followed by acetal removal gave the desired squaraine-fullerene dyad **BE** in good yield under very mild conditions.

Triad photosystem **ABE** was then obtained from **A** by TSE. The templates along the NDI stacks were first removed with excess hydroxylamine following the reported procedures (Figure 1, **X** = **A**). The obtained architecture **A3** was then immersed into a 4 mM solution of dyad **BE** in DMSO for the covalent capture of the aldehydes **BE** by the reactive hydrazides along the NDI stacks in **A3**. The formation of triad photosystem **ABE** by TSE was monitored by absorption spectroscopy. The absorption of the dyad **BE** in solution is dominated by the strong squaraine band at λ_{max} = 660 nm (Figure 4a, dashed). The signature of fullerenes is a steady

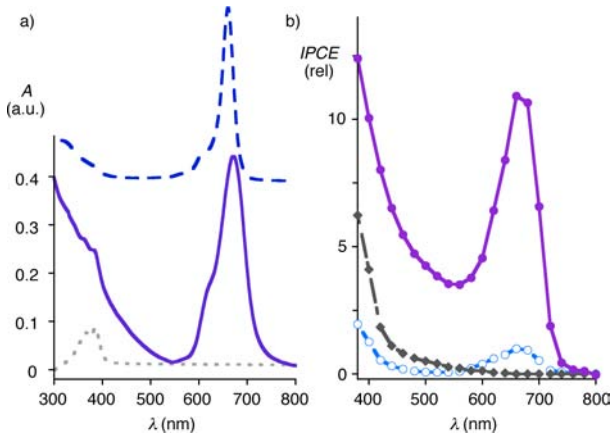

Figure 4. (a) Absorption spectra of dyad **BE** (blue dashed line), single-channel architecture **A3** (gray dotted line), and triple-channel architecture **ABE** (solid purple line). (b) Action spectra of triad architecture **ABE** (solid purple line, filled circles) in comparison to double-channel architectures **AB*** (blue dashed line, empty circles) and **AE** (green hatched line, filled squares). Incident photon-to-current efficiencies (IPCEs) were normalized against that of **AB*** at 660 nm.

increase in absorption beginning around 450 nm. The absorption spectrum of the SOSIP architecture **A3** before TSE shows NDI bands below 400 nm, including partially resolved vibrational finestructures (Figure 4a, dotted). These finestructures are still visible after TSE along with the above-mentioned signatures of squaraines and fullerenes (Figure 4a, solid). Thus, these results indicated the good incorporation of dyads **BE** in the photosystems.

In comparison to the absorbance of NDI before TSE, the absorbance of squaraine at 672 nm was about six times higher. This value was comparable to that obtained by TSE of squaraine **B***. Estimation of TSE yield was complicated by the apparent hypochromism caused by the aggregation[7e] and the sensitivity of squaraines to nucleophiles;[7f] thus yields based on the absorbance values of neither the films nor the films dissolved with 2-mercaptoethanol were meaningful. Therefore, we report here only the yield relative to that of NDI-squaraine double-channel photosystem **AB*** (Table 1). In light of the

Table 1. Summary of Synthesis and Activity of Triad Photosystems

XYZ[a]	MW[b]	shape	yield[c]	J[d]
A		planar		0.1[g]
AB*	892	planar	100%[e]	0.9
ABE	2137	nonplanar	85%[e]	9.9
ABF	1485	planar	82%[e]	0.04
AC*	1426	planar	nd[f]	0.27[g]
ACE	5326	nonplanar	2%	1.1[g]
AD*	802	planar	96%	3.7[g]
ADG	973	nonplanar	92%	9.8[g]
ADH	1034	planarizable	87%	1.2[g]
AD*/G			60%[h]	4.6[g]

[a]For the structure of each component, see Figure 2. The thickness of films was ∼20 nm, estimated on the basis of the absorbance of photosystems **A** (∼0.07 at 380 nm). [b]Molecular weights of stack exchangers. [c]TSE yield. [d]Photocurrent densities (μA cm^{-2}) generated upon irradiation with the simulated sunlight (28 mW cm^{-2}) in the presence of ascorbic acid. [e]TSE yield relative to that of **AB*** system. [f]Not determined. Analogous double-channel system with oxygen-substituted NDI as X gave quantitative yield.[20] [g]TEOA was used instead of ascorbic acid. Lower photocurrents were observed with ascorbic acid. [h]TSE yield of **D*** after 1 day of TSE.

previous observation with large stack exchangers like phthalocyanines, the TSE of smaller and well soluble squaraine **B*** is expected to proceed in nearly quantitative yield. If so, the TSE yield of squaraine-fullerene **BE** calculates to 85%. In any case, similar TSE yield observed for squaraine **B*** and squaraine-fullerene conjugate **BE** demonstrated the remarkable tolerance of TSE to structural variations, and provided support for the existence of triad photosystem **ABE** as depicted in Figure 3. AFM images of triad architecture **ABE** showed characteristic features of SOSIP architectures: smooth surfaces in height images and low-defect long-distance self-organization down toward the molecular level in phase-contrast images (Supporting Information, Figure S4). Thus, evidently the highly ordered structure is intact after TSE with large dyads.

Photocurrent generation was evaluated with the triad photosystem **ABE** as a working electrode, a Pt electrode as cathode, and ascorbic acid as mobile hole acceptor in solution (Figure 5, Table 1). These are very simple, nonoptimized conditions, suited for studies on conceptual innovation from the point of view of supramolecular organic chemistry. Results obtained under identical conditions give trends needed to draw valid conclusions but are naturally not comparable to results from optimized devices.

To assess the significance of triad photosystem **ABE** under these conditions, controls **AB*** with NDI-squaraine dyads and **AE** with NDI-fullerene dyads were therefore prepared by SOSIP-TSE. Gratifyingly, triad photosystem **ABE** generated much more photocurrent than the sum of dyad controls (Figure 5, Table 1). Photocurrent generation could be repeated without significant changes of the kinetic profile. The initial photocurrent decay with triad photosystem **ABE** originates thus from saturation rather than from instability of the photosystem.

dx.doi.org/10.1021/ja405776a | J. Am. Chem. Soc. 2013, 135, 12082−12090

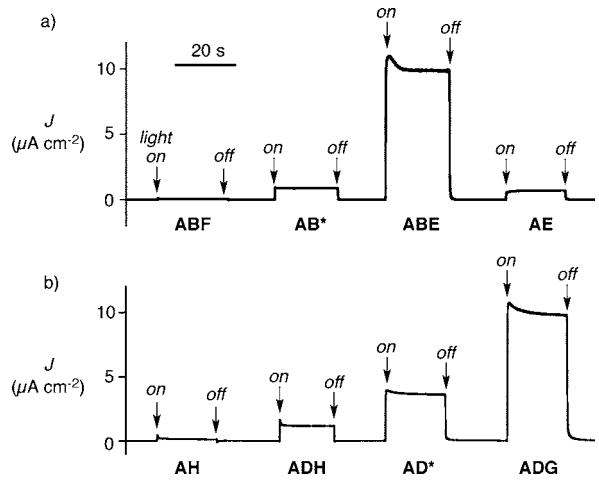

Figure 5. (a) Photocurrent density J generated by triad architectures **ABF** and **ABE** and dyad architectures **AB*** and **AE** in response to irradiation with a solar simulator (power, 28 mW cm^{-2}; 50 mM ascorbic acid; 0.1 M Na_2SO_4 at 0 V vs Ag/AgCl). (b) Same by triad architectures **ADG** and **ADH** and dyad architectures **AD*** and **AH** in response to irradiation with a solar simulator (power, 28 mW cm^{-2}; 50 mM TEOA, 0.1 M Na_2SO_4 at 0 V vs Ag/AgCl).

Similar profiles have been observed previously, but the origin of saturation remains unknown. Charge recombination and poor charge injection into electrode or mobile carrier are reasonable possibilities.

Action spectra report the efficiency of photocurrent generation at specific wavelength and thus reveal the contribution of the individual components. Without strong chromophores, the double-channel photosystem **AE** generated photocurrent only at high energy (Figure 4b◆). Photocurrent generation as such by photosystem **AE** was interesting because it contains only electron transporters, NDI, and fullerenes. Known absence of electron transfer between the two supported their individual contribution to photocurrent generation.[3f] In contrast, double-channel photosystem **AB*** is equipped with excellent electron- and hole-transporting channels. Poor photocurrent generation suggested that charge separation between NDI and squaraine is not efficient, although several other explanations cannot be excluded at this point. Consistent with this explanation, weak IPCE was found for the squaraine chromophore in the action spectrum of photosystem **AB*** (Figure 4b○). In comparison, greatly increased IPCE of squaraines and fullerenes in photosystem **ABE** (Figure 4b●) indicated the improved photoinduced charge separation to be the cause of an overall increased photocurrent, and not only a better light harvesting (Figure 5, Table 1). The significant increase in photocurrent generation from dyad photosystem **AB*** to triad photosystem **ABE** provided a powerful example for the functional relevance of the here-introduced triple-channel architecture (Figures 4b and 5).

Triad Architectures with Squaraines and Core-Expanded NDIs. The core-expanded NDI **F** was considered as replacement of fullerenes **E** in triad architectures. Both are electron acceptors and can transport electrons along their stacks. The LUMO of core-expanded NDI **F** is very low, clearly lower than that of fullerene **E** but also below that of unsubstituted NDIs **A** used in the SOSIP stack (Figure 2, bottom left). Different to fullerene **E**, NDI **F** absorbs strongly at long wavelength.

The target NDI **F**, equipped with a solubilizing alkyl chain and an aldehyde for hydrazone or oxime formation, was synthesized following the procedure reported last year.[16] The squaraine dyad **BF** was prepared by oxime formation and deprotection of the aldehyde as outlined for **BE** (Figure 3). Stack exchange with SOSIP architecture **A** gave triad photosystem **ABF** in high yield (Table 1). However, in sharp contrast to the outstanding performance of **ABE**, photocurrent generation by triad photosystem **ABF** was extremely poor (Figure 5). The addition of the third component **F** inhibited rather than enabled photocurrent generation by double-channel photosystem **AB***.

One possible explanation of the complementary behavior of triad photosystems **ABE** and **ABF** considers that the third component in the former is nonplanar, whereas the one in the latter is planar. With only planar components, triple-channel architectures (Figure 6a) could become unfavorable compared

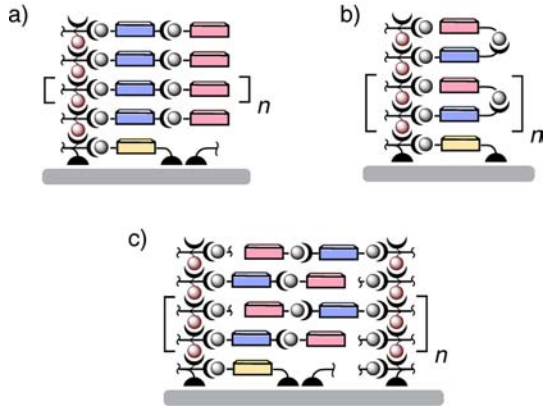

Figure 6. Inactivity of photosystems obtained by SOSIP-TSE with completely planar dyads might indicate the formation of (b) folded or (c) interdigitated donor–acceptor systems rather than (a) triple-channel architectures.

to alternatives with donor–acceptor complexes obtained by folding or interdigitation (Figures 6b,c). Architectures with donor–acceptor complexes should excel with charge separation but suffer from poor charge mobility. They could thus explain the poor photocurrent generation of triad photosystems **ABF** (Figure 5, Table 1). Although other interpretations remain possible (e.g., better charge separation from **B** to **E** than from **B** to **F**), the inactivity of photosystems **ABF** could thus suggest that the TSE-SOSIP with fully planar dyads similar to **BF** does not yield triple-channel architectures but folded or interdigitated alternatives dominated by donor–acceptor complexes.

Triad Architectures with Phthalocyanines and Fullerenes. The excellent yield obtained for the synthesis of triad architecture **ABE** confirmed that TSE tolerates structural changes remarkably well. To explore the limitations of TSE with regard to the size of the stack exchangers, phthalocyanines appeared ideal. Phthalocyanines are the big brothers of squaraines.[7,8] Efficient TSE with simple phthalocyanines **C*** has been achieved previously,[20] but the resulting double-channel architectures (**AC***) produced as little photocurrent as the squaraine analogues **AB*** (Table 1).

Giant stack exchangers **CE** were synthesized to explore the possibility of engineering phthalocyanine–fullerene dyads into triple-channel SOSIP-TSE architectures (Figures 2,7). The phthalocyanine–fullerene stack exchangers **CE** were prepared

dx.doi.org/10.1021/ja405776a | J. Am. Chem. Soc. 2013, 135, 12082–12090

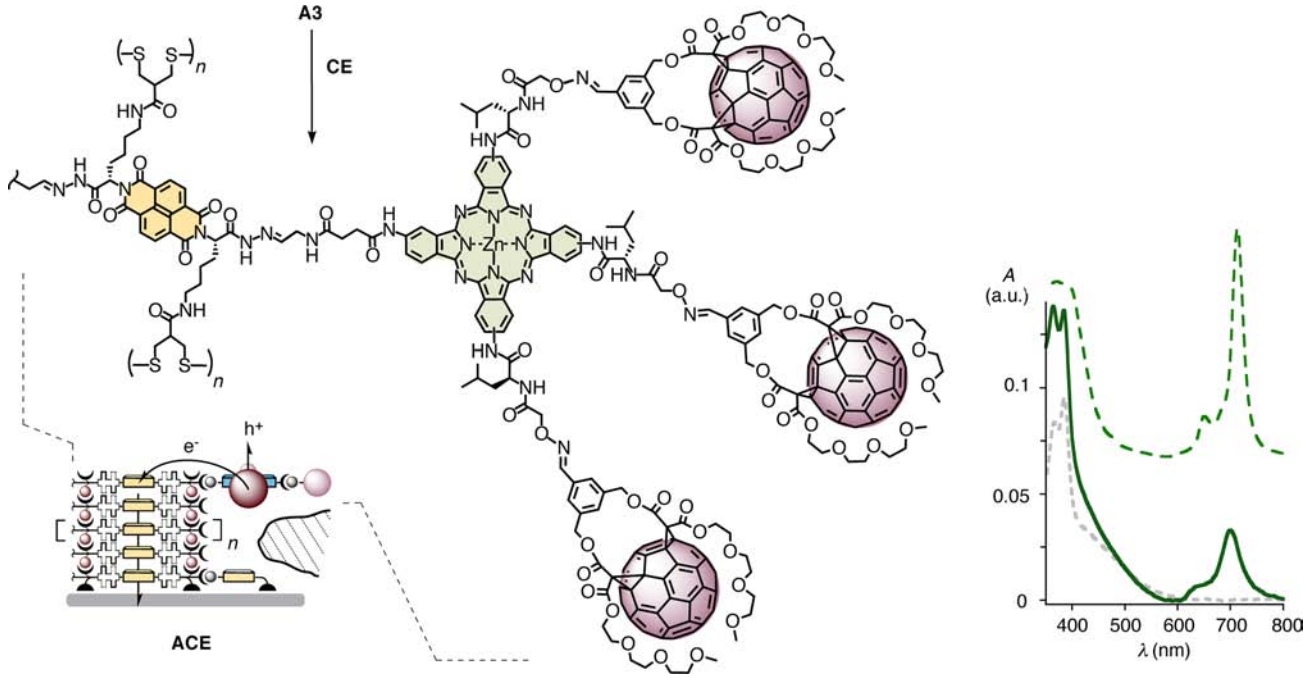

Figure 7. Synthesis and schematic structure of incomplete triad architecture **ACE**, with possible charge-transfer pathways and absorption spectra of dyad **CE** (green dashed line), single-channel architecture **A3** (gray dotted), and incomplete triad architecture **ACE** (green solid).

analogously to the squaraine–fullerene dyads **BE**, using Fmoc rather than Alloc protection of the bifunctional phthalocyanine precursor. The attachment of the three fullerenes **E** and the final aldehyde deprotection to give **CE** were confirmed by MALDI mass spectrometry, whereas NMR spectra of these larger systems were broad in all solvents and thus not very informative. According to the absorption spectra, TSE with the giant exchanger **CE** occurred in only 2% yield (Figure 7). The phthalocyanine band at low energy did also not increase upon disassembly of photosystem **ACE** with 2-mercaptoethanol, thus excluding hypochromism in the solid to obscure better TSE yield.

This poor yield for TSE suggested that the phthalocyanine–fullerene stack exchangers **CE** are too big to enter the pores available along the NDI stacks produced by SOSIP. Most likely, TSE occurs only at the surface of the architectures (Figure 7). Considering this incomplete triple-channel architecture, it was remarkable to find that the presence of the fullerenes in **ACE** nevertheless caused a drastic increase of the global photocurrent compared to double-channel control **AC*** (Table 1). To explain this increase, long-distance electron transfer from fullerenes at the surface to the ITO electrode appeared quite unlikely. Photocurrent generation by the phthalocyanines **C** thus should occur by photoinduced electron transfer first to the fullerene **E** and then from there into the NDI stack for transport to the ITO (Figure 7). The LUMO of NDI **A** below that of fullerene **E** is in agreement with this interpretation. Nevertheless, the most important lesson learned with photosystems **ACE** was that there is an upper limit for SOSIP-TSE; giant stack exchangers are not accepted and react only at the surface.

Triad Architectures with NDIs, PDIs, and Triphenylamines. Among several double-channel architectures tested, photosystem **AD*** generated unusually high photocurrent (Figure 2, Table 1). In this photosystem, a stack of unsubstituted PDIs **D** is introduced by TSE along the original NDI stack obtained by SOSIP. Important for high yielding TSE was the insertion of solubilizing leucines at both sides of the PDI. The high activity of photosystem **AD*** was surprising because stacks of unsubstituted NDIs and PDIs are both known to transport electrons. Inspection of their HOMO and LUMO energy levels suggested that the red PDI stacks in photosystem **AD*** should transport holes rather than electrons (Figure 2, bottom left). Ongoing analysis of this architecture by ultrafast photophysics implies that this interpretation is correct (Vauthey, E.; Sakai, N.; Matile, S., unpublished results). This unusual role of the PDI channels in photosystem **AD*** suggested that the addition of a more conventional hole-transporting channel could give even better activities.

Triphenylamines (TPAs) **G** were selected to explore these triple-channel architectures because their nonplanar, propeller-like structure should disfavor backfolding or interdigitation into inactive donor–acceptor architectures (Figure 6). TSE proceeded in almost quantitative yield to give triad photosystem **ADG** (Figure 2, Table 1). AFM images of **ADG** were consistent with the intact SOSIP architecture (Supporting Information, Figure S4). As expected, the addition of the hole-transporting TPA-channel **G** increased the photocurrent generated by the already quite active double-channel photosystem **AD*** around 2.5 times (Table 1). Improved charge separation was evident in the action spectra, in which the activity of PDIs increased almost four times in triad photosystem **ADG** compared to double-channel photosystem **AD*** (Figure 8a).

Unlike photosystems **ABE** and **AB***, the increase in photocurrent of photosystems **ADG** and **AD*** was not proportional to the increase in IPCE. The explanation of this inconsistency was easily found in the bimolecular recombination loss efficiency η_{BR} (Figure 9).[26] By measuring the dependence of photocurrent on the irradiation power, η_{BR} values of triad systems **ADG** and **ABE** were calculated to be 47% and 3%, respectively. Despite efficient charge separation,

dx.doi.org/10.1021/ja405776a | J. Am. Chem. Soc. 2013, 135, 12082–12090

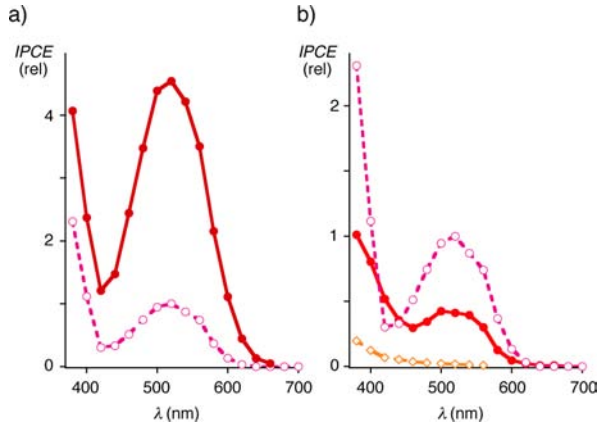

Figure 8. Action spectra of (a) triad architecture **ADG** (filled circles) in comparison to double-channel architectures **AD*** (empty circles) and (b) **ADH** (filled circles) in comparison to **AD*** (empty circles) and **AH** (empty squares). IPCE are normalized relative to that of **AD*** at 520 nm.

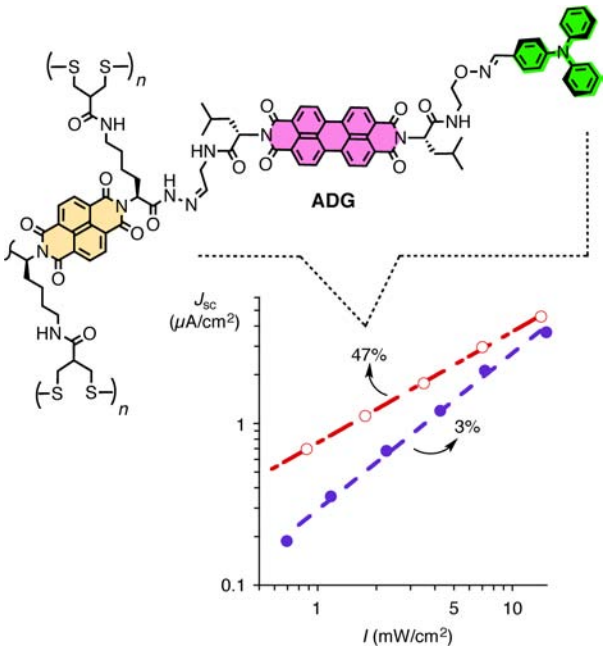

Figure 9. Dependence of short circuit current densities (J_{SC}) on light intensities (I) for triad photosystems **ABE** (purple filled circles) and **ADG** (red empty circles) with bimolecular charge recombination efficiencies η_{BR} indicated in percent.

the relatively high charge recombination in triad system **ADG** reduced the overall photocurrent generation. We interpreted the difference in η_{BR} values to result from different charge mobilities of two systems. Although both are nonplanar, electron-rich triphenylamines do not self-assemble as well as electron-poor fullerenes to give good charge-transporting channels.

As a control experiment, TSE was performed in the presence of the two stack exchangers **D*** and **G** instead of dyad **DG**. As expected from the differences in reactivities and stabilities of aliphatic and aromatic aldehyde hydrazones, fast incorporation of **D*** followed by a slow exchange of **D*** with **G** were observed. Such kinetics should result in the formation of vertically phase-separated second channels composed of mostly pure PDI stacks with TPA stacks only near the surface. Similar photocurrents observed for **AD***/**G** and **AD*** are consistent with this interpretation (Table 1). Thus, these results demonstrated that the organization in photosystem **ADG** is essential for function, that is, provided corroborative evidence for existence and relevance of triple-channel architectures.

Triad Architectures with NDIs, PDIs, and Oligothiophenes. As another class of classical hole transporters, oligothiophenes[5] are generally planar, and their affinity to PDIs is known.[4e] To possibly hinder this donor–acceptor interactions, we chose twisted but planarizable oligothiophene **H**.[5i] Planarity would be eventually desired for better stacking interactions with the other oligothiophenes to secure good charge mobility. To our disappointment, strong affinity between PDI and twisted oligothiophene was already evident during the preparation of **DH**, which was obtained exclusively as a *syn*-oxime isomer. As *anti* is the more stable configuration[22a] and ^{1}H NMR spectra indicated folded conformation, these findings suggested the existence of donor–acceptor type stacking interactions under the reaction conditions. The TSE of PDI-oligothiophene dyads **DH** proceeded in high yield, but the obtained triad photosystem **ADH** generated clearly lower photocurrent compared to the double-channel photosystem **AD*** (Figure 5, Table 1). Action spectra further demonstrated the inactivation of PDIs by the attachment of the oligothiophenes (Figure 8b). Thus, these results provided corroborative evidence for the existence and deactivating effect of donor–acceptor type interactions, which should be dealt with by applying self-sorting principles,[27,18] that is, the introduction of additional elements of molecular recognition which favor the formation of segregated rather than mixed stacks.

CONCLUSIONS

We have shown that triad photosystems are easily accessible by self-organizing surface-initiated polymerization (SOSIP) and templated stack exchange (TSE). The best triad architectures found are composed of NDIs, squaraines, and fullerenes (i.e., **ABE**) or NDIs, PDIs and triphenylamines (i.e., **ADG**). These findings are important because they provide general access to the systematic study of molecular dyads and triads in ordered and oriented multicomponent surface architectures by ultrafast photophysics. Moreover, the disclosed synthetic method might become useful to develop conceptually innovative optoelectronic devices.

Remarkable structural tolerance was found for the synthesis of triad architectures by SOSIP-TSE, and the observed trends are highly consistent and can be rationalized convincingly. Limitations for SOSIP-TSE were discovered only for giant or insoluble stack exchangers (i.e., **ACE**). As expected, photocurrents were greatly improved by the installation of a third component as long as the two chromophores used form separate stacks. This is unproblematic as long as one of the two is not planar (fullerenes in **ABE**, triphenylamines in **ADG**). Photocurrent inhibition indicates that TSE with fully planar donor–acceptor dyads can lead to folded or interdigitated rather than triple-channel architectures (i.e., **ABF**). Relatively weak chromophore deplanarization did not solve the problem, at least not for the oligothiophenes tested (i.e., **ADH**). Considering the confined space available for TSE, preference for folded or interdigitated architectures over the larger triple-channel architectures is reasonable. However, it should be easily possible to suppress folding and interdigitation of planar donor–acceptor dyads by incorporating self-sorting units. Once

dx.doi.org/10.1021/ja405776a | J. Am. Chem. Soc. 2013, 135, 12082–12090

sorting is accomplished, triple-channel architectures seem to be easily accommodated thanks to the not so small space reserved for TSE by two NDI templates per initiator. Moreover, the SOSIP methodology used to build the central stack is not limited to NDIs (e.g., PDIs, oligothiophenes),[15,16] all components of the triad can therefore be quite easily varied. Judged from results with simpler systems,[19,20] the installation of oriented, antiparallel redox gradients in the two channels added by TSE should be very straightforward. Taken together, the results reported in this study demonstrate that the here-introduced triple-channel strategy is a powerful general method to build highly active multicomponent surface architectures of highest sophistication. Interesting topics for the future include the construction of triple-channel systems with refined acceptor−chromophore−donor triads, the expansion toward tetrads and beyond, the prevention of folded and interdigitated architectures (e.g., templated self-sorting),[18] the development of co-TSE (e.g., different kinetics, self-sorting),[18] and so on.

■ ASSOCIATED CONTENT

Supporting Information

Experimental details. This material is available free of charge via the Internet at http://pubs.acs.org.

■ AUTHOR INFORMATION

Corresponding Author

stefan.matile@unige.ch

Present Address

[†]E.O.: Department of Chemistry, Vilnius University, Vilnius, Lithuania.

Notes

The authors declare no competing financial interest.

■ ACKNOWLEDGMENTS

We thank J.-F. Nierengarten (Strasbourg) for advice, A. Fin, H. Shaw, A. Cherix, and D.-H. Tran for contributions to synthesis, D. Jeannerat, A. Pinto, and S. Grass for NMR measurements, the Sciences Mass Spectrometry (SMS) platform for mass spectrometry services, and the University of Geneva, the European Research Council (ERC Advanced Investigator), the National Centre of Competence in Research (NCCR) Chemical Biology, and the Swiss NSF for financial support. E.O. acknowledges a Sciex, G. S. a Curie Fellowship.

■ REFERENCES

(1) (a) Deisenhofer, J.; Michel, H. *Science* **1989**, *245*, 1463−1473. (b) Nelson, N.; Ben-Shem, A. *Nat. Rev. Mol. Cell Biol.* **2004**, *5*, 971−982. (c) Ferreira, K. N. *Science* **2004**, *303*, 1831−1838.

(2) (a) Aida, T.; Meijer, E. W.; Stupp, S. I. *Science* **2012**, *335*, 813−817. (b) Wang, M.; Wudl, F. *J. Mater. Chem.* **2012**, *22*, 24297−24314. (c) Beaujuge, P. M.; Fréchet, J. M. J. *J. Am. Chem. Soc.* **2011**, *133*, 20009−20029. (d) Bassani, D. M.; Jonusauskaite, L.; Lavie-Cambot, A.; McClenaghan, N. D.; Pozzo, J.-L.; Ray, D.; Vives, G. *Coord. Chem. Rev.* **2010**, *254*, 2429−2445. (e) Mei, J.; Diao, Y.; Appleton, A. L.; Fang, L.; Bao, Z. *J. Am. Chem. Soc.* **2013**, *135*, 6724−6746. (f) Guldi, D. M.; Zilbermann, I.; Anderson, G.; Li, A.; Balbinot, D.; Jux, N.; Hatzimarinaki, M.; Hirsch, A.; Prato, M. *Chem. Commun.* **2004**, *40*, 726−727. (g) Bhosale, R.; Míšek, J.; Sakai, N.; Matile, S. *Chem. Soc. Rev.* **2010**, *39*, 138−149.

(3) (a) Bhosale, S. V.; Bhosale, S. V.; Bhargava, S. K. *Org. Biomol. Chem.* **2012**, *10*, 6455−6468. (b) Würthner, F.; Stolte, M. *Chem. Commun.* **2011**, *47*, 5109−5115. (c) Sakai, N.; Mareda, J.; Vauthey, E.; Matile, S. *Chem. Commun.* **2010**, *46*, 4225−4237. (d) Zhan, X.; Facchetti, A.; Barlow, S.; Marks, T. J.; Ratner, M. A.; Wasielewski, M. R.; Marder, S. R. *Adv. Mater.* **2010**, *23*, 268−284. (e) Gao, X.; Di, C.-A.; Hu, Y.; Yang, X.; Fan, H.; Zhang, F.; Liu, Y.; Li, H.; Zhu, D. *J. Am. Chem. Soc.* **2010**, *132*, 3697−3699. (f) El-Khouly, M. E.; Kim, J. H.; Kay, K.-Y.; Choi, C. S.; Ito, O.; Fukuzumi, S. *Chem.—Eur. J.* **2009**, *15*, 5301−5310.

(4) (a) Würthner, F. *Chem. Commun.* **2004**, *40*, 1564−1579. (b) Dössel, L. F.; Kamm, V.; Howard, I. A.; Laquai, F.; Pisula, W.; Feng, X.; Li, C.; Takase, M.; Kudernac, T.; De Feyter, S.; Müllen, K. *J. Am. Chem. Soc.* **2012**, *134*, 5876−5886. (c) Albert-Seifried, S.; Finlayson, C. E.; Laquai, F.; Friend, R. H.; Swager, T. M.; Kouwer, P. H. J.; Juríček, M.; Kitto, H. J.; Valster, S.; Nolte, R. J. M.; Rowan, A. E. *Chem.—Eur. J.* **2010**, *16*, 10021−10029. (d) Mickley Conron, S. M.; Shoer, L. E.; Smeigh, A. L.; Ricks, A. B.; Wasielewski, M. R. *J. Phys. Chem. B* **2013**, *117*, 2195−2204. (e) Li, W.-S.; Saeki, A.; Yamamoto, Y.; Fukushima, T.; Seki, S.; Ishii, N.; Kato, K.; Takata, M.; Aida, T. *Chem. Asian J.* **2010**, *5*, 1566−1572. (f) Sugiyasu, K.; Kawano, S.-I.; Fujita, N.; Shinkai, S. *Chem. Mater.* **2008**, *20*, 2863−2865. (g) Langhals, H.; Böck, B.; Schmid, T.; Marchuk, A. *Chem.—Eur. J.* **2012**, *18*, 13188−13194. (h) Dössel, L. F.; Kamm, V.; Howard, I. A.; Laquai, F.; Pisula, W.; Feng, X.; Li, C.; Takase, M.; Kudernac, T.; De Feyter, S.; Müllen, K. *J. Am. Chem. Soc.* **2012**, *134*, 5876−5886.

(5) (a) Roncali, J. *Acc. Chem. Res.* **2009**, *42*, 1719−1730. (b) Mishra, A.; Ma, C.-Q.; Bäuerle, P. *Chem. Rev.* **2009**, *109*, 1141−1276. (c) di Maria, F.; Gazzano, M.; Zanelli, A.; Gigli, G.; Loiudice, A.; Rizzo, A.; Biasiucci, M.; Salatelli, E.; D'Angelo, P.; Barbarella, G. *Macromolecules* **2012**, *45*, 8284−8291. (d) Kumar, R. J.; MacDonald, J. M.; Singh, T. B.; Waddington, L. J.; Holmes, A. B. *J. Am. Chem. Soc.* **2011**, *133*, 8564−8573. (e) Kamkar, D. A.; Wang, M.; Wudl, F.; Nguyen, T.-Q. *ACS Nano* **2012**, *6*, 1149−1157. (f) Li, W.-S.; Yamamoto, Y.; Fukushima, T.; Saeki, A.; Seki, S.; Tagawa, S.; Masunaga, H.; Sasaki, S.; Takata, M.; Aida, T. *J. Am. Chem. Soc.* **2008**, *130*, 8886−8887. (g) Ramos, A. M.; Rispens, M. T.; van Duren, J. K. J.; Hummelen, J. C.; Janssen, R. A. J. *J. Am. Chem. Soc.* **2001**, *123*, 6714−6715. (h) Miyanishi, S.; Zhang, Y.; Tajima, K.; Hashimoto, K. *Chem. Commun.* **2010**, *46*, 6723−6725. (i) Fin, A.; Vargas Jentzsch, A.; Sakai, N.; Matile, S. *Angew. Chem., Int. Ed.* **2012**, *51*, 12736−12739. (j) Chen, T. L.; Zhang, Y.; Smith, P.; Tamayo, A.; Liu, Y.; Ma, B. *ACS Appl. Mater. Interfaces* **2011**, *3*, 2275−2280. (k) Ie, Y.; Han, A.; Otsubo, T.; Aso, Y. *Chem. Commun.* **2009**, *45*, 3020−3022. (l) Johnson, K.; Huang, Y.-S.; Huettner, S.; Sommer, M.; Brinkmann, M.; Mulherin, R.; Niedzialek, D.; Beljonne, D.; Clark, J.; Huck, W. T. S.; Friend, R. H. *J. Am. Chem. Soc.* **2013**, *135*, 5074−5083 ; compare also references 4e and 4f.

(6) (a) Bonifazi, D.; Enger, O.; Diederich, F. *Chem. Soc. Rev.* **2007**, *36*, 390−414. (b) Guldi, D. M.; Illescas, B. M.; Atienza, C. M.; Wielopolski, M.; Martin, N. *Chem. Soc. Rev.* **2009**, *38*, 1587−1597. (c) Delgado, J. L.; Martin, N.; de la Cruz, P.; Langa, F. *Chem. Soc. Rev.* **2011**, *40*, 5232−5241. (d) Vostrowsky, O.; Hirsch, A. *Chem. Rev.* **2006**, *106*, 5191−5207. (e) Varotto, A.; Treat, N. D.; Jo, J.; Shuttle, C. G.; Batara, N. A.; Brunetti, F. G.; Seo, J. H.; Chabinyc, M. L.; Hawker, C. J.; Heeger, A. J.; Wudl, F. *Angew. Chem., Int. Ed.* **2011**, *50*, 5166−5169. (f) Matsuo, Y.; Oyama, H.; Soga, I.; Okamoto, T.; Tanaka, H.; Saeki, A.; Seki, S.; Nakamura, E. *Chem. Asian J.* **2013**, *8*, 121−128. (g) Imahori, H.; Umeyama, T.; Kurotobi, K.; Takano, Y. *Chem. Commun.* **2012**, *48*, 4032−4045. (h) Urbani, M.; Iehl, J.; Osinska, I.; Louis, R.; Holler, M.; Nierengarten, J.-F. *Eur. J. Org. Chem.* **2009**, *2009*, 3715−3725. (i) Charvet, R.; Yamamoto, Y.; Sasaki, T.; Kim, J.; Kato, K.; Takata, M.; Saeki, A.; Seki, S.; Aida, T. *J. Am. Chem. Soc.* **2012**, *134*, 2524−2527. (j) Mateo-Alonso, A.; Guldi, D. M.; Paolucci, F.; Prato, M. *Angew. Chem., Int. Ed., Engl.* **2007**, *46*, 8120−8126. (k) Matsumoto, F.; Iwai, T.; Moriwaki, K.; Takao, Y.; Ito, T.; Mizuno, T.; Ohno, T. *J. Org. Chem.* **2012**, *77*, 9038−9043. (l) Kitaura, S.; Kurotobi, K.; Sato, M.; Takano, Y.; Umeyama, T.; Imahori, H. *Chem. Commun.* **2012**, *48*, 8550−8552. (m) Hayashi, H.; Nihashi, W.; Umeyama, T.; Matano, Y.; Seki, S.; Shimizu, Y.; Imahori, H. *J. Am. Chem. Soc.* **2011**, *133*, 10736−10739 ; compare also references 5e−h and 5j.

(7) (a) Beverina, L.; Salice, P. *Eur. J. Org. Chem.* **2010**, *2010*, 1207−1225. (b) Park, J.; Barolo, C.; Sauvage, F.; Barbero, N.; Benzi, C.; Quagliotto, P.; Coluccia, S.; Di Censo, D.; Grätzel, M.; Nazeeruddin,

M. K.; Viscardi, G. *Chem. Commun.* **2012**, *48*, 2782−2784. (c) Mayerhöffer, U.; Fimmel, B.; Würthner, F. *Angew. Chem., Int. Ed.* **2012**, *51*, 164−167. (d) Wei, G.; Lunt, R. R.; Sun, K.; Wang, S.; Thompson, M. E.; Forrest, S. R. *Nano Lett* **2010**, *10*, 3555−3559. (e) de Miguel, G.; Ziółek, M.; Zitnan, M.; Organero, J. A.; Pandey, S. S.; Hayase, S.; Douhal, A. *J. Phys. Chem. C* **2012**, *116*, 9379−9389. (f) Ros-Lis, J.; Garcia, B.; Jimenez, D.; Martinez-Manez, R.; Sancenon, F.; Soto, J.; Gonzalvo, F.; Valldecabres, M. *J. Am. Chem. Soc.* **2004**, *126*, 4064−4065. (g) Bagnis, D.; Beverina, L.; Huang, H.; Silvestri, F.; Yao, Y.; Yan, H.; Pagani, G. A.; Marks, T. J.; Facchetti, A. *J. Am. Chem. Soc.* **2010**, *132*, 4074−4075. (h) Völker, S. F.; Renz, M.; Kaupp, M.; Lambert, C. *Chem.—Eur. J.* **2011**, *17*, 14147−14163. (i) Fan, B.; Maniglio, Y.; Simeunovic, M.; Kuster, S.; Geiger, T.; Hany, R.; Nüesch, F. *Int. J. Photoenergy* **2009**, *2009*, 1−7.

(8) (a) Martínez-Díaz, M. V.; la Torre, de, G.; Torres, T. *Chem. Commun.* **2010**, *46*, 7090−7108. (b) Bottari, G.; de la Torre, G.; Guldi, D. M.; Torres, T. *Chem. Rev.* **2010**, *110*, 6768−6816. (c) Walter, M. G.; Rudine, A. B.; Wamser, C. C. *J. Porphyrins Phthalocyanines* **2010**, *14*, 759−792. (d) Göransson, E.; Boixel, J.; Fortage, J.; Jacquemin, D.; Becker, H.-C.; Blart, E.; Hammarström, L.; Odobel, F. *Inorg. Chem.* **2012**, *51*, 11500−11512. (e) Membrino, A.; Paramasivam, M.; Cogoi, S.; Alzeer, J.; Luedtke, N. W.; Xodo, L. E. *Chem. Commun.* **2010**, *46*, 625−627. (f) Yang, F.; Shtein, M.; Forrest, S. *Nat. Mater.* **2005**, *4*, 37−41. (g) O'Sullivan, M. C.; Sprafke, J. K.; Kondratuk, D. V.; Rinfray, C.; Claridge, T. D.; Saywell, A.; Blunt, M. O.; O'Shea, J. N.; Beton, P. H.; Malfois, M.; Anderson, H. L. *Nature* **2011**, *469*, 72−75. (h) Hernández-Eguía, L. P.; Brea, R. J.; Castedo, L.; Ballester, P.; Granja, J. R. *Chem.—Eur. J.* **2011**, *17*, 1220−1229. (i) Ballester, P.; Costa, A.; Deyà, P. M.; Frontera, A.; Gomila, R. M.; Oliva, A. I.; Sanders, J. K. M.; Hunter, C. A. *J. Org. Chem.* **2005**, *70*, 6616−6622. (j) Kim, D.; Osuka, A. *Acc. Chem. Res.* **2004**, *37*, 735−745 compare also refs 4c and 6g.

(9) (a) Brennan, B. J.; Liddell, P. A.; Moore, T. A.; Moore, A. L.; Gust, D. *J. Phys. Chem. B* **2013**, *117*, 426−432. (b) Yella, A.; Lee, H. W.; Tsao, H. N.; Yi, C.; Chandiran, A. K.; Nazeeruddin, M. K.; Diau, E. W. G.; Yeh, C. Y.; Zakeeruddin, S. M.; Grätzel, M. *Science* **2011**, *334*, 629−634 Compare also refs 4d and 6g−i.

(10) (a) Snaith, H. J.; Whiting, G. L.; Sun, B.; Greenham, N.; Huck, W. T. S.; Friend, R. H. *Nano Lett* **2005**, *5*, 1653−1657. (b) Lambert, C.; Ehbets, J.; Rausch, D.; Steeger, M. *J. Org. Chem.* **2012**, *77*, 6147−6154. (c) Faramarzi, V.; Niess, F.; Moulin, E.; Maaloum, M.; Dayen, J.-F.; Beaufrand, J.-B.; Zanettini, S.; Doudin, B.; Giuseppone, N. *Nat. Chem.* **2012**, *4*, 485−490.

(11) (a) Sakai, N.; Sisson, A. L.; Bürgi, T.; Matile, S. *J. Am. Chem. Soc.* **2007**, *129*, 15758−15759. (b) Sakai, N.; Bhosale, R.; Emery, D.; Mareda, J.; Matile, S. *J. Am. Chem. Soc.* **2010**, *132*, 6923−6925.

(12) (a) Sakai, N.; Lista, M.; Kel, O.; Sakurai, S.-I.; Emery, D.; Mareda, J.; Vauthey, E.; Matile, S. *J. Am. Chem. Soc.* **2011**, *133*, 15224−15227. (b) Lista, M.; Areephong, J.; Sakai, N.; Matile, S. *J. Am. Chem. Soc.* **2011**, *133*, 15228−15231.

(13) Bang, E.-K.; Lista, M.; Sforazzini, G.; Sakai, N.; Matile, S. *Chem. Sci.* **2012**, *3*, 1752−1763.

(14) Luh, T.-Y. *Acc. Chem. Res.* **2013**, *46*, 378−389.

(15) Charbonnaz, P.; Sakai, N.; Matile, S. *Chem. Sci.* **2012**, *3*, 1492−1496.

(16) Areephong, J.; Orentas, E.; Sakai, N.; Matile, S. *Chem. Commun.* **2012**, *48*, 10618−10620.

(17) Bolag, A.; Hayashi, H.; Charbonnaz, P.; Sakai, N.; Matile, S. *ChemistryOpen* **2013**, *2*, 55−57.

(18) Orentas, E.; Lista, M.; Lin, N.-T.; Sakai, N.; Matile, S. *Nat. Chem.* **2012**, *4*, 746−750.

(19) (a) Sakai, N.; Matile, S. *J. Am. Chem. Soc.* **2011**, *133*, 18542−18545. (b) Sakai, N.; Matile, S. *Beilstein J. Org. Chem.* **2012**, *8*, 897−904.

(20) Sforazzini, G.; Turdean, R.; Sakai, N.; Matile, S. *Chem. Sci.* **2013**, *4*, 1847−1851.

(21) (a) Rodriguez-Docampo, Z.; Otto, S. *Chem. Commun.* **2008**, *44*, 5301−5303. (b) von Delius, M.; Geertsema, E. M.; Leigh, D. A. *Nat. Chem.* **2010**, *2*, 96−101. (c) Barrell, M. J.; Campa, A. G.; von Delius, M.; Geertsema, E. M.; Leigh, D. A. *Angew. Chem., Int. Ed.* **2011**, *50*, 285−290.

(22) (a) Corbett, P. T.; Leclaire, J.; Vial, L.; West, K. R.; Wietor, J. L.; Sanders, J. K. M.; Otto, S. *Chem. Rev.* **2006**, *106*, 3652−3711. (b) Otto, S. *Acc. Chem. Res.* **2012**, *45*, 2200−2210. (c) Cougnon, F. B. L.; Sanders, J. K. M. *Acc. Chem. Res.* **2012**, *45*, 2211−2221. (d) Lehn, J.-M. *Top. Curr. Chem.* **2012**, *322*, 1−32.

(23) Würthner, F.; Chen, Z.; Hoeben, F. J. M.; Osswald, P.; You, C.; Jonkheijm, P.; Herrikhuyzen, von, J.; Schenning, A. P. H. J.; van der Schoot, P.; Meijer, E. W.; Beckers, E.; Meskers, S.; Janssen, R. A. J. *J. Am. Chem. Soc.* **2004**, *126*, 10611−10618 compare refs 2−12, 15−20.

(24) (a) Grimm, B.; Schornbaum, J.; Jasch, H.; Trukhina, O.; Wessendorf, F.; Hirsch, A.; Torres, T.; Guldi, D. M. *Proc. Natl. Acad. Sci. U.S.A.* **2012**, *109*, 15565−15571. (b) Megiatto, J. D.; Antoniuk-Pablant, A.; Sherman, B. D.; Kodis, G.; Gervaldo, M.; Moore, T. A.; Moore, A. L.; Gust, D. *Proc. Natl. Acad. Sci. U.S.A.* **2012**, *109*, 15578−15583. (c) Karsten, B. P.; Smith, P. P.; Tamayo, A. B.; Janssen, R. A. J. *J. Phys. Chem. A* **2012**, *116*, 1146−1150. (d) Narutaki, M.; Takimiya, K.; Otsubo, T.; Harima, Y.; Zhang, H.; Araki, Y.; Ito, O. *J. Org. Chem.* **2006**, *71*, 1761−1768. (e) Steinberg-Yfrach, G.; Liddell, P.; Hung, S.; Moore, A. M.; Gust, D.; Moore, T. A. *Nature* **1997**, *385*, 239−241.

(25) (a) Iha, R. K.; Wooley, K. L.; Nyström, A. M.; Burke, D. J.; Kade, M. J.; Hawker, C. J. *Chem. Rev.* **2009**, *109*, 5620−5686. (b) Kalia, J.; Raines, R. T. *Angew. Chem., Int. Ed.* **2008**, *47*, 7523−7526.

(26) Koster, L. J. A.; Kemerink, M.; Wienk, M. M.; Maturová, K.; Janssen, R. A. J. *Adv. Mater.* **2011**, *23*, 1670−1674.

(27) Safont-Sempere, M. M.; Fernández, G.; Würthner, F. *Chem. Rev.* **2011**, *111*, 5784−5814.